SSRG International Journal of Electronics and Communication Engineering
ISSN: 2348-8549/ https://doi.org/10.14445/23488549/IJECE-V11I8P105

Volume 11 Issue 8, 42-54, August 2024

Original Article

Feature Based Fusion Model for Automated Detection of Brain Diseases from MRI Images

M. Chengathir Selvi[1], R. Jaya Swathika[2], K.T.R. Thivyasree[3]

[1,2,,3]*Department of Computer Science and Engineering, Mepco Schlenk Engineering College (Autonomous), Tamil Nadu, India.*

[1]*Corresponding Auhtor : chengathir@gmail.com*

Received: 29 May 2024 Revised: 12 July 2024 Accepted: 06 August 2024 Published: 31 August 2024

Abstract - *Due to the increasing rate of disease afflictions among people lately, the need for automatic illness diagnosis systems is more imperative. Most of the automatic illness diagnosis systems aim to support the physician in disease screening and decision-making. Furthermore, an immense amount of research is done on the human brain, a complicated and important organ, using imaging methods like Magnetic Resonance Imaging (MRI) to look at brain activity and uncover abnormalities. When compared to other imaging modalities, MRI stands out for its superior soft tissue contrast and safety profile. This research aims to develop a computer-aided disease diagnosis system to classify brain MRI images with high accuracy. The research significantly contributes to the following: developing an ensemble model based on deep learning and proposing a new feature selection technique that employs a framework of rank-based correlation and entropy. The framework's final step uses an ensemble learning process to classify the extracted features. The stages of the suggested framework are as follows: (i) gathering and resizing images; (ii) deep feature extraction using the pre-trained networks; (iii) handcrafted feature extraction; (iv) serial feature concatenation; (v) finest feature selection using entropy and rank-based correlation and (vi) classification using a voting classifier. The suggested approach intends to improve the effectiveness and accuracy of brain disease diagnosis, opening the door for early detection and prompt intervention by integrating MRI imaging modality and AI algorithms. Experimental investigations conducted using MATLAB software demonstrate promising results in the preprocessing of MRI pictures and the detection of brain diseases through the proposed fusion model by achieving an accuracy of 89.87%. The findings of this study emphasize the significance of AI-based approaches in automated brain disease detection, offering a valuable contribution to the field of medical imaging and diagnostics.*

Keywords - *Fusion model, Feature based, MRI, Machine Learning, Entropy, Rank-based correlation.*

1. Introduction

The brain is the most valuable and intricate organ in the human body. Medical imaging methods to study brain activity and detect abnormalities include Positron Emission Tomography (PET), Computed Tomography (CT), and Magnetic Resonance Imaging (MRI). Among these, MRI provides the highest soft tissue contrast without using ionizing radiation. It utilizes a magnetic field and radio waves to generate highly detailed images of the brain and its structures. Moreover, MRI is a non-invasive and painless technique. In clinical practice, MRI is the most commonly used imaging method for the brain, offering significant advantages such as strong contrast between soft tissues. However, interpreting MRI scans remains a labour-intensive, time-consuming, and error-prone process in medical practice.

Interpreting MRI scans is a tedious, time-consuming, and error-prone process in medical practice. Moreover, significant experience is required for the sensitive and accurate detection of diseases like Alzheimer's and tumors. Therefore, to automate the diagnosis of various brain illnesses from MRI images, an AI-based model is necessary. The Shearlet Subband Energy Feature-Based Individual Network utilizes Structural Magnetic Resonance Imaging (sMRI) to identify Alzheimer's Disease (AD) [1]. This method employs the automated anatomical labelling atlas to create 90 Regions of Interest (ROIs) from the sMRI image, constructing the network. Directional subband-based energy feature vectors represent each ROI.

Over the past decade, significant advancements in Machine Learning and Artificial Intelligence have captivated financial institutions, businesses, and academia. This progress is largely driven by deep artificial neural networks, also known as deep learning. Siamese networks have been shown to function similarly to research using whole-brain MR images, with the added benefits of reduced computing complexity and time [2]. In the realm of medical imaging analysis, deep learning-enabled algorithms are delivering remarkable results and are seen as essential for future applications. These algorithms can process medical imaging data sets to provide accurate and efficient diagnoses. In

medical imaging analytics, deep learning is critical for tasks such as image segmentation, registration, and disease diagnosis. However, some models construct a brain network using only spatial domain-based features, overlooking the frequency domain-based features of the Regions of Interest (ROIs) [1].

The novel AI-based fusion model introduced in this work enhances the efficiency of automatic MRI image-based diagnosis for brain illnesses such as Alzheimer's, brain tumors, atrophy, ischemia, and White Matter Intensity (WMI). This deep learning model assists specialists by reducing their workload and the tedious process of analyzing and interpreting radiological images. Despite their impressive capabilities, AI models have several drawbacks, including their susceptibility to dataset heterogeneity. The data used for training AI systems is crucial for generating accurate predictions or classifications. Consequently, when the training dataset differs significantly from real-world data, a dataset bias or dataset shift occurs, potentially compromising the AI model's performance. The ADNI and BIOCARD datasets were used to evaluate the effectiveness of the Siamese network approach; however, it remains uncertain whether these results are applicable to other datasets or populations [2].

Despite advances in medical imaging technology, interpreting brain scans remains challenging. A major obstacle is the variability in brain architecture and diseases among individuals. Human brains differ significantly in size, shape, and structure, making it difficult to develop universally applicable diagnostic algorithms. This can lead to inflated performance metrics during evaluation but poor performance in real-world applications. Additionally, not all healthcare facilities possess the expertise needed to identify subtle anomalies in brain scans. These challenges underscore the need for reliable and adaptable AI models to support accurate and efficient interpretation of brain imaging data. However, feature ranking and classification error techniques may inadvertently select features or parameters that perform well on the training data but fail to generalize to new, unseen data [3]. Therefore, it is crucial to leverage the benefits of cross-validation.

The main objectives are listed as follows:

- Extract deep features and handcrafted features using pre-trained and local texture descriptors.
- Classify the MRI images using the most significant and frequently used classifiers.
- Horizontal concatenation of feature vectors extracted by the pre-trained and handcrafted feature extractors that got high accuracy.
- Select the best features using Entropy and Rank Correlation.
- Use a voting classifier to detect the presence of brain disease.

2. Related Works

The paper by Zeng A et al. [4] initially performed a systematic and critical review of the state-of-the-art methods for classifying Alzheimer's disease using convolutional neural networks and T1-weighted MRI. They then introduced an open-source framework for reproducible evaluation of classification approaches. In this study, a fivefold cross-validation procedure was rigorously followed and repeated ten times for each binary experiment, namely AD vs. HC, MCIc vs. HC, and MCIc vs. MCInc.

In the methodology used by Venugopalan et al. [5], intermediate features generated from different imaging modalities are integrated using a concatenation layer, followed by a classification layer to predict the stage of Alzheimer's disease. The study explores various classifiers for the classification layer, including K-Nearest Neighbors (KNN), decision trees, random forests, and Support Vector Machines (SVM).

The study also employs deep learning models like auto-encoders and deep-belief networks for fusing PET and MRI image data, resulting in improved predictions. To address the challenge of small sample sizes, the study proposes strategies such as transfer learning and domain adaptation.

The study by Xin Bi et al. [6] employed two deep learning methods for brain network classification: a convolutional learning method to learn deep regional-connectivity features and a recurrent learning method to learn deep adjacent positional features. Additionally, an ELM-boosted structure was implemented to enhance the models' learning ability. The number of hidden nodes in the ELM varied from 0 to 300, with performance metrics such as accuracy, recall, and AUC being measured. Considering both performance and training time, the final ELM was set to have 150 hidden nodes.

Guo and Zhang [7] proposed an Improved Deep Learning Algorithm (IDLA) for the early detection of Alzheimer's disease, utilizing a specialized network of autoencoders to differentiate between natural aging and disease progression. The study used resting-state functional MRI data to measure connectivity in brain regions and assess brain function.

The IDLA approach integrates effectively biased neural network functionality, enhancing the reliability of Alzheimer's disease recognition. Compared to conventional classifiers, the proposed deep learning algorithm demonstrated significant improvement, reducing the standard deviation by 45% and indicating a more reliable and efficient forecasting model.

The study by Siar et al. [8] employed a Convolutional Neural Network (CNN) for detecting brain tumors using MRI images. The CNN achieved an accuracy of 98.67% with the Softmax Fully Connected layer for image classification. Additionally, the study utilized the Radial Basis Function

(RBF) classifier and the Decision Tree (DT) classifier alongside the CNN. The CNN with the RBF classifier reached an accuracy of 97.34%, while the CNN with the DT classifier achieved 94.24%. The study introduced a novel method that integrates feature extraction techniques with CNN for tumor detection, achieving an accuracy of 99.12% on the test data.

The paper by Ramzan et al. [9] utilized Residual Neural Networks (ResNet-18 architecture) for feature extraction and classification across multiple stages of Alzheimer's disease. The study investigated the effectiveness of using resting-state functional magnetic resonance imaging (rs-fMRI) for multi-class classification of Alzheimer's Disease (AD) and its stages, offering a potential tool for early diagnosis.

The models were trained from scratch using single-channel input, and transfer learning was applied both with and without fine-tuning using an extended network architecture. The model achieved state-of-the-art results, with average accuracies of 97.92% for off-the-shelf models and 97.88% for fine-tuned models.

The paper by Duc et al. [10] utilized resting-state functional Magnetic Resonance Imaging (rs-fMRI) scans from 331 participants to generate functional 3-Dimensional (3-D) independent component spatial maps for classification and regression tasks. They developed a 3-D Convolutional Neural Network (CNN) architecture for the classification task.

To enhance MMSE regression performance, feature optimization methods such as least absolute shrinkage and selection operator and Support Vector Machine-based Recursive Feature Elimination (SVM-RFE) were applied. A permutation test was conducted to evaluate the statistical significance of the 3-D CNN classifier's performance.

In the paper by Zhu et al. [11], a hybrid model architecture was developed to leverage both types of clinical data. This model integrates transfer learning-based convolutional neural networks for MRI scans with a fully connected deep learning neural network for symptom data. Three models were created: one based solely on symptoms, one based solely on MRI scans, and a hybrid model combining both data sources.

The symptoms-based model employed a fully connected deep learning neural network, while both the MRI scans-only and hybrid models utilized transfer learning-based convolutional neural networks. Among these, the hybrid model, which integrated both symptom data and MRI scans, achieved the highest accuracy of 0.94, demonstrating its effectiveness in accurately diagnosing Parkinson's disease.

The paper by Wutao Yin et al. [12] employs deep learning techniques, specifically Convolutional Neural Networks (CNNs) and Recurrent Neural Networks (RNNs), to analyze fMRI data for diagnosing brain disorders. The fMRI data is treated as images, time series, or image series, with various deep learning models developed to process the data for different tasks. The study highlights the successful application of these deep learning methods for diagnosing brain disorders based on fMRI images.

The paper by Tian Bai et al. [13] introduces a novel three-component adversarial network-based method for Alzheimer's Disease (AD) detection called BSGAN-ADD. This method combines Generative Adversarial Network (GAN)-based Brain Slice Image Enhancement with Deep Convolutional Neural Network (CNN)-based AD detection.

During the training phase, the generator in BSGAN-ADD incorporates disease category feedback from the classifier to improve 2D brain slice image reconstruction, with constraints provided by the discriminator. In the prediction phase, stacked CNN layers in the generator are used to extract high-level brain features from the enhanced 2D brain slice images, which are then used by the classifier to determine the posterior probabilities of different disease states (Normal, AD, and MCI).

In [14], the authors fused Computed Tomography (CT) and MRI scans to create new synthetic images with enriched information, which could enhance diagnostic accuracy. Image segmentation techniques were used to improve tumor identification. Building on this, [15] introduced a novel model based on Generative Adversarial Networks (GANs) for enhanced segmentation.

Additionally, [16] proposed a Convolutional Neural Network (CNN)-based model for normalized segmentation to identify tumor regions. A review by the authors in [17] examined both supervised and unsupervised deep learning techniques for tumor identification. Furthermore, [18] analyzed tumor growth using various machine learning algorithms for segmenting multiparametric MRI (mpMRI) images.

Rajnikanth et al. [19] developed a Computer-Aided Diagnosis and Detection (CADD) system that utilizes Convolutional Neural Network (CNN)-supported segmentation and classification to identify glioblastoma and glioma-class brain tumors in 2D MRI slices. The effectiveness of the CADD system was validated through testing on benchmark and real clinical brain MRI slices, with a comparison of various well-known classifiers. They found that the SVM-Cubic classifier achieved the highest accuracy, exceeding 98%. These results highlight that CNN-assisted segmentation and classification can significantly enhance disease detection accuracy.

Numerous promising machine learning applications have utilized MRI for Alzheimer's Disease (AD) prediction [20]. These applications include methods such as Random Forests (RF) [21], Support Vector Machines (SVM) [22], and boosting algorithms [23]. In recent years, numerous studies

have utilized CNN-based tumor identification algorithms and deep learning fusion models in medical imaging to improve the accuracy of diagnosing complex brain disorders such as Alzheimer's disease. By integrating MRI and fMRI data into their analyses, researchers have achieved significant advancements in identifying these conditions, demonstrating considerable progress in the field of neuroimaging.

3. Proposed Methodology

This paper introduces an innovative AI-driven fusion model that significantly improves the effectiveness of automating the diagnosis of various brain disorders, including but not limited to Alzheimer's disease, brain tumors, atrophy, ischemia, and White Matter Intensity (WMI). By leveraging advanced artificial intelligence techniques, this model streamlines the process of interpreting MRI images, allowing for more accurate and timely identification of crucial brain abnormalities that could greatly benefit patient outcomes and medical decision-making.

The objectives of this study are as follows:

- To extract deep and handcrafted features from pre-trained models and local texture descriptors.
- To classify the images using frequently utilized classifiers.
- To select the best features using Entropy and Rank Correlation-based feature selector.
- To detect the presence of brain illness using a voting classifier.

To accomplish the above specified objectives, an AI-based fusion model to detect the presence of brain diseases like Atrophy, Ischemia, White Matter Intensity (WMI), Brain Tumors and Alzheimer's is proposed. For developing this model, a Brain MRI image Dataset from various sources is acquired. To enhance the quality of the images, preprocessing on the given data set is performed. The features are extracted using pre-trained and handcrafted feature extractors.

The pre-trained and handcrafted extracted features are used for classification. To improve the accuracy, the optimal features are identified from both types of extractors mentioned earlier and the corresponding feature vectors are concatenated horizontally. Based on Entropy and Rank correlation, the best features are selected. Finally, the resulting optimized features are trained using a voting classifier to detect the brain disease. Figure 1 depicts the overall process of the model.

3.1. Preprocessing

Preprocessing is done through sharpening and cropping the brain MRI images. Sharpening is done by adding the original image and the image after the edge detection to produce a new image where the edges are enhanced, making it look sharper. Medical images can benefit from sharpening procedures that improve the edges and small details, making subtle abnormalities more noticeable and detectable. Sharpening can increase the visibility of appropriate characteristics in brain imaging, where the identification of minute lesions or anomalies is essential for diagnosis. This increases the precision of disease detection algorithms.

Cropping is done by removing unwanted parts of the sharpened image to focus on the most relevant features. It is necessary to provide consistency among datasets, standardise the size and orientation of medical images, and enable automated analysis. Preprocessing can help reduce computing overhead during future processing steps by removing unnecessary information from images and cropping them to focus on the region of interest, such as the brain.

By increasing the visibility of significant anatomical structures and disease characteristics, preprocessing procedures like sharpening and cropping can improve the interpretability of medical images. Finally, only the brain is stripped from the original image. The process is represented in Figure 2.

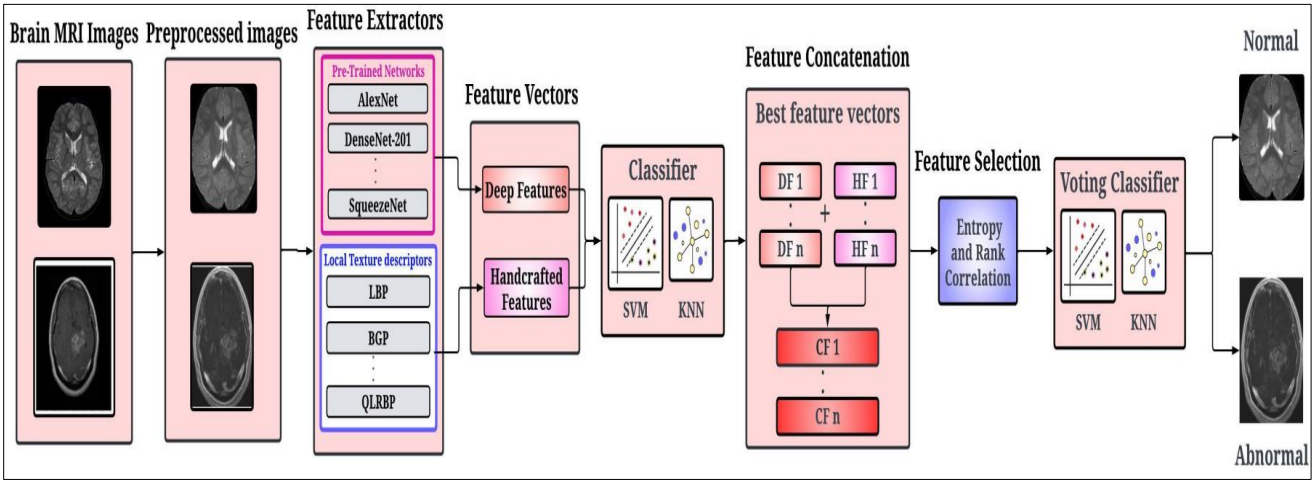

Fig. 1 Proposed system design for brain tumor classification

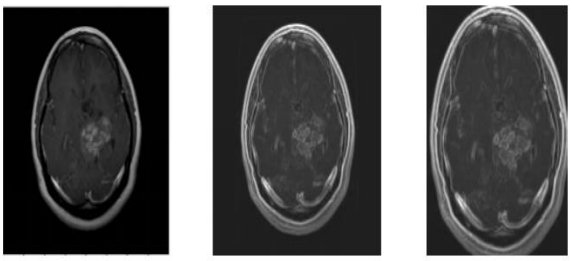

Original Image Sharpened Image Cropped Image

Fig. 2 Transition from original to preprocessed images

3.2. Deep Feature Extraction

Eight well-known pre-trained CNN models, AlexNet, DenseNet201, GoogleNet, VGG16, MobileNetV2, ResNet50, ResNet101, and SqueezeNet, were used for this purpose, and their features were taken without any fine-tuning. From every pre-trained CNN model, a total of 8435 × 1000-sized features were extracted, with 1000 features extracted for every preprocessed MRI image.

The features that were taken out of every pretrained CNN model were then assessed using 10-fold cross-validation on traditional classifiers. TFrom low-level features like edges and textures to high-level semantic characteristics like object categories, these pre-trained algorithms have learned to extract hierarchical information from images fed. The algorithm represented in Algorithm 1 shows from which layer the features are extracted from the respective pre-trained feature extractor.

Algorithm 1: Pseudocode for Feature Extraction Using Pre-Trained Models

Output : $PF_8 \leftarrow$ Extracted Features
Input : $\psi(i, j, k) \leftarrow$ Input Images

$PF_1 \leftarrow$ Extract_Features (‘AlexNet’, ‘FC8’, ?)
$PF_2 \leftarrow$ Extract_Features (‘DenseNet201’, ‘FC1000’, ?)
$PF_3 \leftarrow$ Extract_Features (‘GoogleNet’, ‘Loss3-Classifier’, ?)
$PF_4 \leftarrow$ Extract_Features (‘VGG16’, ‘FC8’, ?)
$PF_5 \leftarrow$ Extract_Features (‘MobileNetV2’, ‘Logits’, ?)
$PF_6 \leftarrow$ Extract_Features (‘ResNet50’, ‘FC1000’, ?)
$PF_7 \leftarrow$ Extract_Features (‘ResNet101’, ‘FC1000’, ?)
$PF_8 \leftarrow$ Extract_Features (‘SqueezeNet’, ‘Pool10’, ?)

3.3. Handcrafted Feature Extraction

Using a variety of local texture descriptors, handcrafted features were extracted in order to compare with deep features and build an accurate ensemble model. Eight well-known local texture descriptors Local Binary Pattern (LBP), Frequency Decoded Local Binary Pattern (FDLBP), Pyramid Histogram of Oriented Gradients (PHOG), Binary Gabor Pattern (BGP), Census Transform Histogram (CENTRIST), Binarized Statistical Image Features (BSIF), Quaternionic Local Ranking Binary Pattern (QLRBP), and Local Phase Quantization (LPQ) were utilized for this purpose. The extracted characteristics were assessed by a 10-fold cross-validation technique using traditional classifiers. The algorithm is represented in Algorithm 2 shows from which local texture descriptors the features are extracted and in which variables they are stored.

Algorithm 2: Pseudocode for Feature Extraction Using Pre-Trained Models

Output : $HF_8 \leftarrow$ Extracted Features
Input : $?(i, j, k) \leftarrow$ Input Images

$HF_1 \leftarrow$ Extract_Features (‘LBP’, ?)
$HF_2 \leftarrow$ Extract_Features (‘FDLBP’, ?)
$HF_3 \leftarrow$ Extract_Features (‘PHOG’, ?)
$HF_4 \leftarrow$ Extract_Features (‘BGP’, ?)
$HF_5 \leftarrow$ Extract_Features (‘CENTRIST’, ?)
$HF_6 \leftarrow$ Extract_Features (‘BSIF’, ?)
$HF_7 \leftarrow$ Extract_Features (‘QLRBP’, ?)
$HF_8 \leftarrow$ Extract_Features (‘LPQ’, ?)

Because LBP, FDLBP, and LPQ are resistant to variations in illumination, they operate consistently, even under a variety of lighting scenarios that are frequently encountered in medical imaging. Rotation-invariant texture patterns are captured by PHOG, QLRBP, and LPQ, guaranteeing that significant features associated with brain structures can be identified regardless of the orientation of the pictures.

Fuzzy logic and interpretable feature representations are incorporated by FDLBP and CENTRIST, respectively, to improve the derived features' discriminative ability and enable more precise brain illness categorization. By combining local data into global representations, BGP and BSIF are resistant to spatial variability and deformations found in brain images, which variations in imaging techniques or patient placement may bring on.

3.4. Classification

The deep features and handcrafted features undergo classification using seven prominent classifiers known as Cubic SVM, Gaussian SVM, Fine KNN, Weighted KNN, Bagged Tree, Boosted Tree, and Subspace KNN. These classifiers are specifically chosen for their ability to capture complex correlations present in brain imaging data effectively. They encompass a diverse set of modeling strategies, including subspace-based, ensemble methods like Bagged Tree and Boosted Tree, non-linear techniques such as KNN, and linear algorithms like SVM.

Noteworthy among these classifiers are Boosted Tree, Bagged Tree, and Gaussian SVM, which excel in detecting subtle irregularities and intricate patterns that are indicative of

various brain disorders. This capability plays a crucial role in facilitating the process of diagnosis and treatment planning for healthcare professionals.

Furthermore, ensemble classifiers like Boosted Tree and Bagged Tree leverage the combined knowledge of multiple models to combat overfitting, enhance generalization performance, and fortify the reliability of brain disease detection models. Moreover, Subspace-based classifiers such as Subspace KNN mitigate issues related to high dimensionality by employing feature subspace selection techniques, thereby optimizing nearest neighbor searches through a focus on the most relevant features in the data.

3.5. Feature Concatenation

The feature vectors extracted by the best pre-trained model and the best handcrafted model are concatenated horizontally, effectively augmenting the dimensionality of the resulting feature vectors. This strategic concatenation approach merges diverse types of features originating from various regions or modalities within brain MRI images by seamlessly integrating high-level semantic features from pre-trained models with fine-grained textural details derived through handcrafted approaches, a synergistic depiction unfolds, offering a holistic view of brain pathology.

This comprehensive framework captures intricate nuances of brain morphology, surface textures, and functional connectivity patterns. Consequently, this fusion of detailed insights enables a nuanced understanding of brain anatomy and pathology, covering a spectrum of attributes ranging from overarching structural characteristics to subtle textural cues. The amalgamation of these distinctive feature types facilitates a robust characterisation of brain structures and abnormalities, enriching the analysis with a blend of semantic richness and granular detail, thereby advancing the capacity for in-depth brain assessment and diagnosis.

Masterfully crafted feature extractors are designed with the precise intention of identifying and isolating distinctive patterns and characteristics that are specific to a given domain, particularly in the realm of brain imaging. Through the strategic utilization of horizontal concatenation, domain-specific information is effectively harnessed by merging these extracted features with the knowledge acquired by pre-trained models from more general image datasets. This strategic amalgamation serves to enhance the discriminatory power of the feature representation, which is particularly beneficial for tasks that involve the detection and diagnosis of various brain-related ailments.

Handcrafted feature extractors focus on diligently capturing intricate textural motifs and essential structural elements, while pre-trained deep learning algorithms are proficient in learning complex hierarchical representations of visual data. By amalgamating insights from these complementary sources, horizontal concatenation operates at its peak potential, amplifying the depth and diversity of the feature space while bolstering the overall robustness and generalizability of the classification model. In essence, leveraging both these methods not only enriches the feature space but also reinforces the model's ability to classify with accuracy across different brain imaging scenarios.

Horizontal concatenation, which involves intentionally combining features acquired through diverse methods, serves to maintain the clarity and comprehension of each feature element. By uniting these varied features, one can gain valuable insights into the foundational attributes that impact the process of classification.

This insight into the discriminative capabilities of different types of features promotes collaboration between machine learning experts and specialists in the realm of brain disease research. Through this transparency, the task of comprehending and harnessing the diverse potentials of various feature categories becomes more accessible, facilitating effective cooperation and knowledge sharing among practitioners and experts in the field.

3.6. Feature Selection

A variety of classification techniques, including cubic SVM, gaussian SVM, fine KNN, weighted KNN, bagged tree, boosted tree, and subspace KNN, are applied to classify the features derived from both handcrafted and pre-trained feature extractors. The feature vectors of the two highly accurate feature extractors are chosen: one from the pre-trained set and the other from the handcrafted feature extractors. The two chosen feature extractors' feature vectors are fused horizontally.

Following the fusion process, the combined feature vectors undergo a selection process using entropy measures and rank correlation techniques. A method that considers both rank correlation and the entropy values of the fused vector is employed to refine the selection of the feature vectors. This innovative approach enhances the accuracy and robustness of the classification process by leveraging the complementary information captured through the fusion and selection steps.

The recommended approach consists of three basic steps:

- Figuring out the fused features' entropy value,
- Calculating the correlation between them
- Selecting the features with the lowest entropy-correlation values.

After computing the entropy value of the fused feature and multiplying it by the rank correlation, the subsequent step involves applying a threshold function to ascertain which features exhibit the lowest entropy correlation value. This meticulous process of entropy-based feature selection proves invaluable as it allows for the identification of features with strong discriminatory capabilities, ones that are resilient to interference from noise or irrelevant data components.

Additionally, the utilization of the rank correlation methodology serves to pinpoint those features that exhibit a pronounced correlation with the target variable, thereby enhancing their relevance in the final classification. Once these meticulously selected features have undergone assessment and refinement, they are subsequently channeled into the voting classifier for the conclusive stage of classification. This systematic approach ensures that the classification process is underpinned by a robust framework, leading to more accurate and reliable outcomes.

It is given that extracted fused features f_1, f_2, ...f_n are ranked from 1 to n. Find out the correlation between the rank of given features. The rank correlation is defined as:

$$R_f = \frac{n\Sigma f_1 f_2 - \Sigma f_1 f_2}{\sqrt{n\sum f_1^2 - (\Sigma f_1)^2 (n\sum f_2^2 - (\Sigma f_2)^2)}} \quad (1)$$

Where, f_1 and f2 represent the fused feature vector. On simplifications (1) becomes:

$$R_f = 1 - \left(\frac{6\sum d^2}{n^3 - n}\right) \quad (2)$$

Where $\sum d^2 = \Sigma(f)_1^2 + \sum (f_2)^2 - 2\Sigma f_1 f_2$. Then, calculate the entropy value of the fused feature vector and multiply it with the correlation. The obtained value is compared with each feature of the fused vector, and the features are based on the final threshold function as follows:

$$\text{EC } (f_i) = \text{Entropy} \times 1 - \left(\frac{6\sum d^2}{n^3 - n}\right) \quad (3)$$

$$\overrightarrow{F_{(VeC)}} = \begin{cases} Remove_i fi > EC(fi) \\ Select_i\ f_i \leq EC(f_i) \end{cases} \quad (4)$$

Resultant vector $\overrightarrow{F_{(VeC)}}$ is utilized for final classification.

Algorithm 3: Pseudocode for Entropy and Rank Correlation based Feature Selection

Output : $\overrightarrow{F_{(VeC)}} \leftarrow$ Selected Features
Input : Pretrained Features $_8$, Handcrafted Features $_8$

FV1=0
FV2=0
For (j: 1 to 8)
V1 ← Pretrained Features(j)
If (acc(V1) > FV1)
FV1= V1
End For

For (j: 1 to 8)
V2 ← Handcrafted Features(j)
If (acc(V2)>FV2)
FV2= V2
End For

Fused(Fv)← [FV1 , FV2]
Calculate the Entropy of Fused(Fv)
For (m: 1 to no_of_features)
Rank Correlation (RC) ← $1 - \left(\frac{6\sum d^2}{n^3 - n}\right)$
EC = Entropy × RC
If (Fv(i) <= EC)
$\overrightarrow{F_{(VeC)}} \leftarrow [\overrightarrow{F_{(VeC)}}, \text{Fv(i)}]$
End For

The suggested approach involves carefully identifying the most effective features to enhance the classification process. This entails computing the entropy and rank-based correlation scores of the fused features during the feature selection phase. By considering both entropy and rank-based correlation, the technique aims to eliminate feature redundancy and prioritize the selection of the most relevant features for accurate classification. Algorithm 3 outlines the detailed procedure for this feature selection process, underscoring the methodical approach taken to ensure the best feature subset is chosen for precise classification outcomes. Such a methodical process not only improves the accuracy of the classification but also streamlines the model for better performance in handling complex datasets.

Initially, two variables, FV1 and FV2, are set to 0 and designated to hold the features extracted from both the pretrained and handcrafted feature extractors, respectively. The process begins by iterating through the pretrained features to identify and store the feature with the highest accuracy (acc) in the variable FV1. Similarly, the algorithm then proceeds to iterate through the handcrafted features, preserving the feature with the highest accuracy (acc) in the variable FV2. Following this selection process, the algorithm merges the chosen features, FV1 and FV2, together into a unified set named Fused(Fv) by combining them through horizontal concatenation. This combined set is then subjected to an entropy calculation, aiming to quantify the level of uncertainty or disorder inherent within the amalgamated selected features, Fused(Fv).

Moving forward, for each specific feature within the fused set, the algorithm proceeds to assess its Rank Correlation (RC) before calculating the product of Entropy and one minus rank Correlation (EC). By comparing this product against the feature's value, the algorithm determines whether the feature should be included in the final output of selected features if its value is less than or equal to EC. This meticulous selection process ensures that only the most relevant and impactful features are retained for further analysis and utilization.

3.7. Voting Classification

The exemplary study exhaustively utilized a distinguished set of seven classifiers for the in-depth analysis: Cubic Support Vector Machine (SVM), Gaussian SVM, Fine

K-Nearest Neighbors (KNN), Weighted KNN, Bagged Tree, Boosted Tree, and Subspace KNN. These diverse classifiers were thoughtfully employed to meticulously examine and compare the impact of both the intricately extracted deep features and the manually crafted features, all in pursuit of achieving a thorough and all-encompassing classification outcome. Through a diligent and detailed evaluation procedure, the most precise and effective classifiers were carefully pinpointed to form an integral part of the ensemble technique known as the voting classifier.

This deliberate fusion of the most accurate classifiers notably enhanced the overall system's operational efficiency and trustworthiness, thereby spotlighting the critical role of a well-planned and meticulously executed selection process in steering classification results to higher levels of excellence and dependability.

4. Expermental Results

The study extensively employed seven notable classifiers for the analysis: Cubic SVM, Gaussian SVM, Fine KNN, Weighted KNN, Bagged Tree, Boosted Tree, and Subspace KNN. These classifiers were thoughtfully applied to scrutinize both the deep features and handcrafted features in order to achieve a comprehensive classification.

Following a meticulous evaluation process, the most accurate classifiers were deliberately selected to contribute to the ensemble method known as the voting classifier. This strategic integration of superior classifiers notably boosted the system's overall performance and reliability, showcasing the effectiveness of a well-thought-out selection process in enhancing classification outcomes.

4.1. Dataset Collection

The datasets utilized in this study consist of a total of 444 T2-W MRI images in JPG format. Specifically, there are 100 images for atrophy, 92 for WMI, 102 for ischemia, and 150 for the normal class. For the brain tumor dataset, there are a total of 2870 training images, with 395 images representing 'No tumor' and 2475 images depicting 'Tumor', along with 394 testing images, split as 105 'No tumor' and 289 'Tumor'. In the case of the Alzheimer's dataset, a total of 5121 images are designated for training purposes and 1279 images for testing. Each class is visually illustrated using the raw MRI images, as shown in Figure 3, with additional detailed information provided in Table 1 regarding the dataset.

Table 1. Databases, number of files, classes, colors, and format

Database	Files	Classes	Color	Format
Tumor	3264	3	Grayscale	jpg
Alzheimer's	6400	3	Grayscale	jpg
Atrophy, Ischemia	444	4	Grayscale	jpg

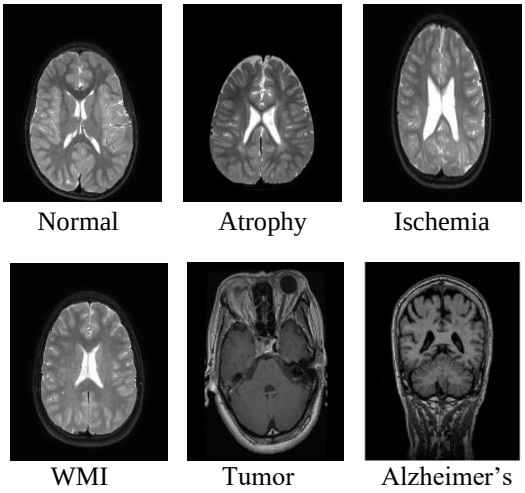

Fig. 3 MRI images

4.2. Deep Feature Extraction

The classification results of pre-trained models are shown in Table 2. DenseNet consistently earns the greatest average accuracy (81.24%) among all pre-trained models, with MobileNetV2 coming in a close second (81.08%). This suggests that these pre-trained models are efficient at accurately classifying brain illnesses by extracting relevant data from brain MRI images. Given the great performance of pre-trained models such as DenseNet and MobileNetV2, it appears that brain disease diagnosis can benefit from transfer learning.

Pre-trained models are effective in medical imaging tasks; these models have learnt generic properties related to brain image classification. When using the same classifiers with various pre-trained models, there is variation in performance. For example, among most classifiers, DenseNet gets the maximum accuracy, but in certain situations, models like ResNet50 and ResNet101 perform marginally worse. This implies that the pre-trained model selection can affect the total classification accuracy, emphasising how crucial it is to choose the right model for the given task.

Furthermore, it seems that KNN-based classifiers (Weighted KNN and Fine KNN) perform on par with, and sometimes even better than, tree-based ensemble techniques (Bagged Tree and Boosted Tree). For instance, Fine KNN outperforms Bagged Tree (62.0%) and Boosted Tree (63.3%) in terms of accuracy when applied to the DenseNet pre-trained model.

Similarly, Fine KNN outperforms Bagged Tree (59.5%) and Boosted Tree (72.3%) with an accuracy of 93.7% using the MobileNetV2 pre-trained model. This suggests that KNN-based classifiers can indeed offer competitive or even better performance than tree-based ensemble approaches in the context of brain illness detection using the features derived from pre-trained deep learning models.

4.3. Handcrafted Feature Extraction

For the purpose of extracting distinguishing characteristics from brain MRI pictures, local texture descriptors are essential. The classification results of handcrafted feature extractors are shown in Table 3. The goal of these descriptors, which include PHOG, CENTRIST, FDLBP, and LBP, is to describe the texture patterns found in the MRI images, which can reveal information about underlying brain diseases and architecture. Different local texture descriptors function differently from one another. Certain descriptors are successful in capturing relevant textural information for the identification of brain diseases, as evidenced by their consistently high accuracies across classifiers. PHOG and FDLBP, for instance, perform well across a range of classifiers, indicating their resilience and discriminating ability.

Table 2. Accuracy scores were obtained using conventional classifiers with features extracted from various pretrained models

Pretrained Model	Cubic SVM	Gaussian SVM	Fine KNN	Weighted KNN	Bagged Tree	Boosted Tree	Subspace KNN
PHOG	94	75.2	93.8	90	63.8	57.7	94.21
CENTRIST	65.8	55.9	62.2	65.7	57.3	64.7	81.9
FDLBP	92.2	83.3	96.8	93	61.44	73	97
LBP	91.5	80.8	95	91.8	59.8	72.3	94.7
BGP	95.4	68.9	78	85.5	60.8	78	93.4
LPQ	95.5	70.2	93	86	62.4	76.9	93
BSIF	95.6	68.8	91.1	87.3	63.6	72.9	92.1
QLRBP	89.7	69	92.5	88.8	57.1	77.7	92.7

Table 3. Accuracy scores were obtained using conventional classifiers with features extracted from various handcrafted models

Pretrained Model	Cubic SVM	Gaussian SVM	Fine KNN	Weighted KNN	Bagged Tree	Boosted Tree	Subspace KNN
Alexnet	91.7	67.4	93.02	88.6	66.03	60.9	92.6
Googlenet	86.7	66.3	88.7	83.11	59.22	60.8	88.3
DenseNet	93.3	71.3	94.4	89.9	62	63.3	**94.5**
MobileNetV2	90.5	70.4	93.7	87.5	59.5	72.3	93.7
SqueezeNet	91.4	67.8	91.7	86.6	59.8	73	91.6
ResNet50	91.5	69.1	92.2	85.9	61	73.6	92.3
ResNet101	91.6	68.7	92.4	86.7	60.3	72.9	92.1
VGG16	88.7	66.7	91.3	85.5	59.7	71.7	91.1

The classifier selection strongly influences the performance of local texture descriptors. Certain descriptors exhibit classifier sensitivity, whilst others function well across a range of classifiers. As an example, CENTRIST performance varies throughout classifiers, suggesting that the classifier's capacity to utilize the extracted texture characteristics may be a determining factor in the success of the model. Certain combinations of classifiers and local texture descriptors perform better than others every time. When combined with KNN models like Subspace KNN and Fine KNN, descriptors like FDLBP and LBP continually yield excellent accuracies, demonstrating the resilience and efficacy of these combinations for the identification of brain diseases.

4.4. Evaluation Metrics

A confusion matrix is a table that helps us understand how well a machine learning model is performing. It is used to evaluate classification models, which are used to categorize data into different classes based on certain features or characteristics. The table has four components: true positives, false positives, true negatives, and false negatives.

True Positives (TP) are the cases where the model correctly identifies a positive outcome. For example, in a spam email filter, a true positive is an email that was correctly identified as spam. False Positives (FP) are the cases where the model incorrectly identifies a positive outcome. In a spam email filter example, a false positive is an email that was

incorrectly identified as spam. True Negatives (TN) are the cases where the model correctly identifies a negative outcome. For instance, in a medical diagnosis model, a true negative is a healthy patient who was correctly identified as healthy. Finally, False Negatives (FN) are the cases where the model incorrectly identifies a negative outcome. In the disease diagnosis model, a false negative is a diseased brain which was wrongly identified as healthy.

Figures 4, 5, 6 and 7 display the confusion matrix of the topmost classifier as well as the topmost pertained model and local feature extractors, i.e., DenseNet and FDLBP for the combined dataset. The diagonal cells (blue-backed and highlighted) in Figure 4 display the number of accurate predictions for each class. For instance, Atrophy was predicted by the model 96 times, Ischemia 93 times, MildDemented 713 times, and so forth. For every class, these are referred to as true positives.

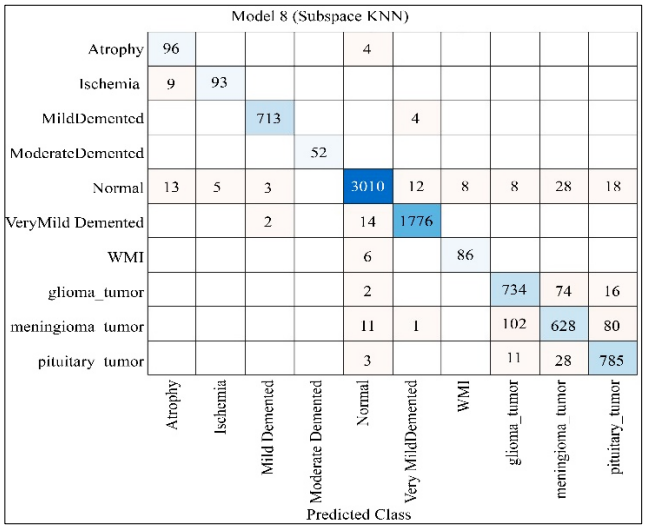

Fig. 4 Confusion matrix of DenseNet of classifier Subspace KNN

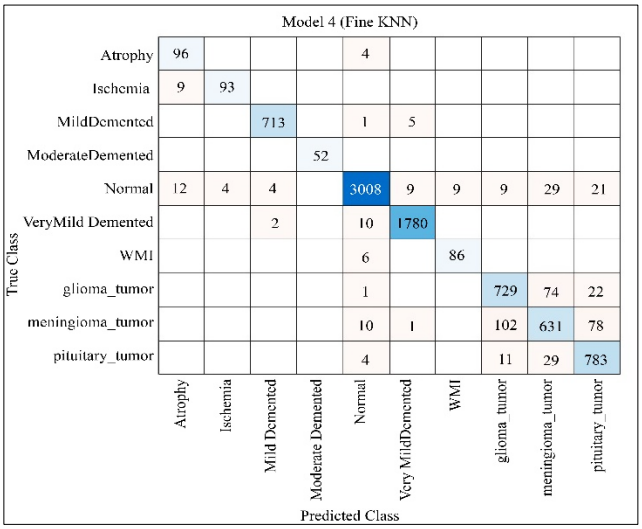

Fig. 5 Confusion matrix of DenseNet of classifier Fine KNN

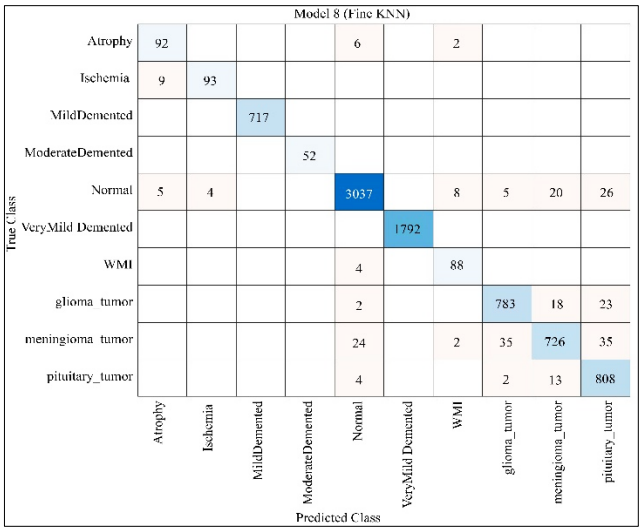

Fig. 6 Confusion matrix of FDLBP of classifier Subspace KNN

The number of inaccurate predictions, i.e., predictions made by the model that deviates from the actual class, is displayed in the off-diagonal cells. For example, the model predicted 13 images of Normal as Atrophy and 9 images of Ischemia as Atrophy.

In Figure 5, for instance, Atrophy was predicted by the model 96 times, Ischemia 93 times, MildDemented 711 times, and so forth. The model predicted 12 images of Normal as Atrophy and 9 images of “Ischemia” as “Atrophy”. Similarly, in Figure 6, for instance, Atrophy was predicted by the model 92 times, Ischemia 93 times, MildDemented 717 times, and so forth. The model predicted 5 images of Normal as Atrophy and 9 images of Ischemia as Atrophy. In the same way in Figure 7, for instance, Atrophy was predicted by the model 94 times, Ischemia 93 times, MildDemented 717 times, and so forth. The model predicted 5 images of Normal as Atrophy and 9 images of Ischemia as Atrophy.

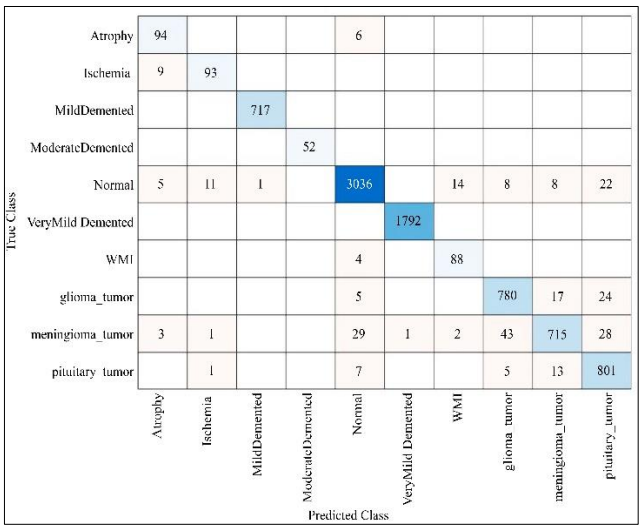

Fig. 7 Confusion matrix of FDLBP of classifier Fine KNN

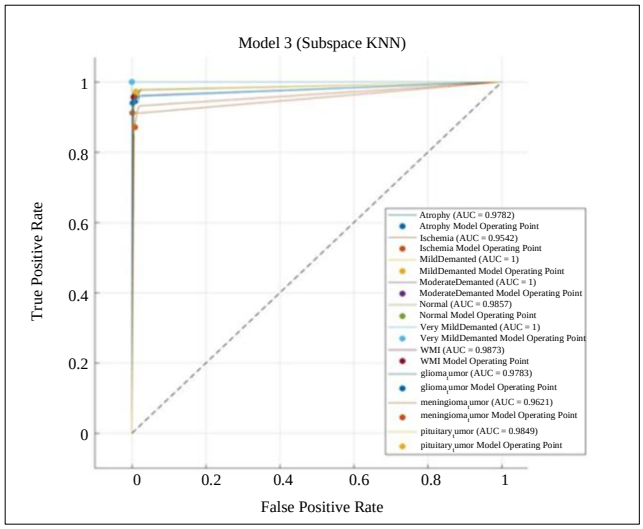

Fig. 8 AUC curve for Subspace KNN of FDLBP

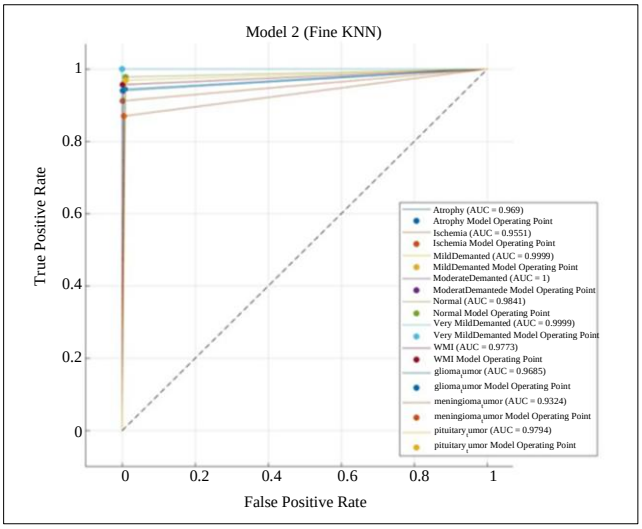

Fig. 9 AUC curve for Fine KNN of FDLBP

When assessing the effectiveness of classification models in medical imaging tasks like categorizing brain MRI pictures into distinct disorders, one typical statistic to utilize is the Area under the Curve (AUC). Plotting the true positive rate (sensitivity) versus the false positive rate (1-specificity) at different threshold settings is the AUC curve, additionally referred to as the Receiver Operating Characteristic (ROC) curve. The AUC quantifies the overall performance of the classification model. A higher AUC value (closer to 1) indicates better discrimination ability, meaning the model is better at distinguishing between positive and negative cases. An AUC of 0.5 suggests random classification, while an AUC of 1 indicates perfect classification.

5. Conclusion

Since MRI can give great contrast to soft tissues, it is frequently used to examine the human brain and discover problems. However, the process of studying and interpreting MRI scans is arduous and time-consuming for specialists. In addition, misinterpretations may arise from time constraints in cases where professionals are overworked. Artificial intelligence is developing at a rapid pace, especially in deep learning, which has produced creative answers to these problems. In this study, a novel deep learning model for classifying brain MRI images according to brain illnesses is presented. For feature extraction, the suggested model uses one local texture descriptor, FDLBP, together with one deep model, DenseNet. The combined deep and hand-crafted features are then sent into the suggested feature selection method.

The model's high accuracy scores suggest that it can be used as a clinical adjunct tool to help specialists accurately classify brain MRI images based on brain diseases. It automatically selects the best-performing feature subset and nearest neighbor value. It also uses cubic SVM, Fine KNN, and Subspace KNN to classify the most important features that were selected. Using the ADNI, Atropy, Ischemia, WMI and brain tumor datasets, the model achieved an accuracy of 89.87%.

Acknowledgments

The author would like to express his heartfelt gratitude to the Principal and HoD/CSE, Mepco Schlenk Engineering College, for their guidance and unwavering support during this research.

References

[1] Dan Pan et al., "Early Detection of Alzheimer's Disease Using Magnetic Resonance Imaging: A Novel Approach Combining Convolutional Neural Networks and Ensemble Learning," *Frontiers in Neuroscience*, vol. 14, pp. 1-19, 2020. [CrossRef] [Google Scholar] [Publisher Link]

[2] Janani Venugopalan et al., "Multimodal Deep Learning Models for Early Detection of Alzheimer's Disease Stage," *Scientific Reports*, vol. 11, no. 1, pp. 1-13, 2021. [CrossRef] [Google Scholar] [Publisher Link]

[3] Xin Bi et al., "Functional Brain Network Classification for Alzheimer's Disease Detection with Deep Features and Extreme Learning Machine," *Cognitive Computation*, vol. 12, pp. 513-527, 2020. [CrossRef] [Google Scholar] [Publisher Link]

[4] Haibing Guo, and Yongjin Zhang, "Resting State fMRI and Improved Deep Learning Algorithm for Earlier Detection of Alzheimer's Disease," *IEEE Access*, vol. 8, pp. 115383-115392, 2020. [CrossRef] [Google Scholar] [Publisher Link]

[5] Masoumeh Siar, and Mohammad Teshnehlab, "Brain Tumor Detection Using Deep Neural Network and Machine Learning Algorithm," *2019 9th International Conference on Computer and Knowledge Engineering*, Mashhad, Iran, pp. 363-368, 2019. [CrossRef] [Google Scholar] [Publisher Link]

[6] Farheen Ramzan et al., "A Deep Learning Approach for Automated Diagnosis and Multi-Class Classification of Alzheimer's Disease Stages Using Resting-State fMRI and Residual Neural Networks," *Journal of Medical Systems*, vol. 44, pp. 1-16, 2019. [CrossRef] [Google Scholar] [Publisher Link]

[7] Nguyen Thanh Duc et al., "3D-Deep Learning Based Automatic Diagnosis of Alzheimer's Disease with Joint MMSE Prediction Using Resting-State fMRI," *Neuroinformatics*, vol. 18, pp. 71-86, 2020. [CrossRef] [Google Scholar] [Publisher Link]

[8] Sabrina Zhu, "Early Diagnosis of Parkinson's Disease by Analyzing Magnetic Resonance Imaging Brain Scans and Patient Characteristic," *2022 10th International Conference on Bioinformatics and Computational Biology*, Hangzhou, China, pp. 116-123, 2022. [CrossRef] [Google Scholar] [Publisher Link]

[9] Wutao Yin, Longhai Li, and Fang-Xiang Wu, "Deep Learning for Brain Disorder Diagnosis Based on fMRI Images," *Neurocomputing*, vol. 469, pp. 332-345, 2022. [CrossRef] [Google Scholar] [Publisher Link]

[10] Tian Bai et al., "A Novel Alzheimer's Disease Detection Approach Using GAN-Based Brain Slice Image Enhancement," *Neurocomputing*, vol. 492, pp. 353-369, 2022. [CrossRef] [Google Scholar] [Publisher Link]

[11] Shah Rukh Muzammil et al., "CSID: A Novel Multimodal Image Fusion Algorithm for Enhanced Clinical Diagnosis," *Diagnostics*, vol. 10, no. 11, pp. 1-22, 2020. [CrossRef] [Google Scholar] [Publisher Link]

[12] Jiwoong J. Jeong et al., "Systematic Review of Generative Adversarial Networks (GANs) for Medical Image Classification and Segmentation," *Journal of Digital Imaging*, vol. 35, pp. 137-152, 2022. [CrossRef] [Google Scholar] [Publisher Link]

[13] Ahmet Ilhan, Boran Sekeroglu, and Rahib Abiyev, "Brain Tumor Segmentation in MRI Images Using Nonparametric Localization and Enhancement Methods with U-Net," *International Journal of Computer Assisted Radiology and Surgery*, vol. 17, pp. 589-600, 2022. [CrossRef] [Google Scholar] [Publisher Link]

[14] Tanzila Saba, "Recent Advancement in Cancer Detection Using Machine Learning: Systematic Survey of Decades, Comparisons and Challenges," *Journal of Infection and Public Health*, vol. 13, no. 9, pp. 1274-1289, 2020. [CrossRef] [Google Scholar] [Publisher Link]

[15] Spyridon Bakas et al., "Identifying the Best Machine Learning Algorithms for Brain Tumor Segmentation, Progression Assessment, and Overall Survival Prediction in the BRATS Challenge," *arXiv*, 2019. [CrossRef] [Google Scholar] [Publisher Link]

[16] Venkatesan Rajinikanth, Seifedine Kadry, and Yunyoung Nam, "Convolutional-Neural-Network Assisted Segmentation and SVM Classification of Brain Tumor in Clinical MRI Slices," *Information Technology and Control*, vol. 50, no. 2, pp. 342-356, 2021. [CrossRef] [Google Scholar] [Publisher Link]

[17] José María Mateos-Pérez et al., "Structural Neuroimaging as Clinical Predictor: A Review of Machine Learning Applications," *NeuroImage: Clinical*, vol. 20, pp. 506-522, 2018. [CrossRef] [Google Scholar] [Publisher Link]

[18] Evanthia E. Tripoliti, Dimitrios I. Fotiadis, and Maria Argyropoulou, "A Supervised Method to Assist the Diagnosis and Monitor Progression of Alzheimer's Disease Using Data from an fMRI Experiment," *Artificial Intelligence in Medicine*, vol. 53, no. 1, pp. 35-45, 2011. [CrossRef] [Google Scholar] [Publisher Link]

[19] K. Van Leemput et al., "Automated Model-Based Tissue Classification of MR Images of the Brain," *IEEE Transactions on Medical Imaging*, vol. 18, no. 10, pp. 897-908, 1999. [CrossRef] [Google Scholar] [Publisher Link]

[20] Chris Hinrichs et al., "Spatially Augmented LPboosting for AD Classification with Evaluations on the ADNI Dataset," *NeuroImage*, vol. 48, no. 1, pp. 138-149, 2009. [CrossRef] [Google Scholar] [Publisher Link]

[21] Sunil L. Bangare, "Classification of Optimal Brain Tissue Using Dynamic Region Growing and Fuzzy Min-Max Neural Network in Brain Magnetic Resonance Images," *Neuroscience Informatics*, vol. 2, no. 3, pp. 1-9, 2022. [CrossRef] [Google Scholar] [Publisher Link]

[22] Anna Bosch, Andrew Zisserman, and Xavier Muñoz, "Representing Shape with a Spatial Pyramid Kernel," *Proceedings of the 6th ACM International Conference on Image and Video Retrieval*, Amsterdam The Netherlands, pp. 401-408, 2007. [CrossRef] [Google Scholar] [Publisher Link]

[23] Daban Abdulsalam Abdullah, Muhammed H. Akpınar, and Abdulkadir Şengür, "Local Feature Descriptors Based ECG Beat Classification," *Health Information Science and Systems*, vol. 8, 2020. [CrossRef] [Google Scholar] [Publisher Link]

[24] Lin Zhang, Zhiqiang Zhou, and Hongyu Li, "Binary Gabor Pattern: An Efficient and Robust Descriptor for Texture Classification," *2012 19th IEEE International Conference on Image Processing*, Orlando, FL, USA, pp. 81-84, 2012. [CrossRef] [Google Scholar] [Publisher Link]

[25] Jianxin Wu, and Jim M. Rehg, "CENTRIST: A Visual Descriptor for Scene Categorization," *IEEE Transactions on Pattern Analysis and Machine Intelligence*, vol. 33, no. 8, pp. 1489-1501, 2011. [CrossRef] [Google Scholar] [Publisher Link]

[26] Juho Kannala, and Esa Rahtu, "BSIF: Binarized Statistical Image Features," *Proceedings of the 21st International Conference on Pattern Recognition (ICPR2012)*, Tsukuba, Japan, pp. 1363-1366, 2012. [Google Scholar] [Publisher Link]

[27] Rushi Lan, Yicong Zhou, and Yuan Yan Tang, "Quaternionic Local Ranking Binary Pattern: A Local Descriptor of Color Images," *IEEE Transactions on Image Processing*, vol. 25, no. 2, pp. 566-579, 2016. [CrossRef] [Google Scholar] [Publisher Link]

[28] Ville Ojansivu, and Janne Heikkilä, "Blur Insensitive Texture Classification Using Local Phase Quantization," *Image and Signal Processing, Lecture Notes in Computer Science*, vol. 5099, pp. 236-243, 2008. [CrossRef] [Google Scholar] [Publisher Link]

[29] Ahmad Alsahaf et al., "A Framework for Feature Selection through Boosting," *Expert Systems with Applications*, vol. 187, pp. 1-10, 2022. [CrossRef] [Google Scholar] [Publisher Link]

[30] Mehrdad Rostami et al., "Review of Swarm Intelligence-Based Feature Selection Methods," *Engineering Applications of Artificial Intelligence*, vol. 100, 2021. [CrossRef] [Google Scholar] [Publisher Link]

[31] Igor Kononenko, "Estimating Attributes: Analysis and Extensions of RELIEF," *Machine Learning: ECML-94, Lecture Notes in Computer Science*, vol. 784, pp. 171-182, 1994. [CrossRef] [Google Scholar] [Publisher Link]

[32] Kenji Kira, and Larry Arthur Rendell, "The Feature Selection Problem: Traditional Methods and a New Algorithm," *Proceedings of the Tenth National Conference on Artificial Intelligence*, San Jose California, pp. 129-134, 1992. [Google Scholar] [Publisher Link]

[33] Sartaj, Brain Tumor Classification (MRI), Kaggle. [Online]. Available: https://www.kaggle.com/datasets/sartajbhuvaji/brain-tumor-classification-mri

[34] Suravi Akhter et al., "A Relief Based Feature Subset Selection Method," *Dhaka University Journal of Applied Science and Engineering*, vol. 6, no. 2, pp. 7-13, 2021. [CrossRef] [Google Scholar] [Publisher Link]

[35] Bruce Draper, Carol Kaito, and Jose Bins, "Iterative Relief," *2003 Conference on Computer Vision and Pattern Recognition Workshop*, Madison, WI, USA, pp. 62-62, 2003. [CrossRef] [Google Scholar] [Publisher Link]

[36] Yijun Sun, and Jiandong Li, "Iterative Relief for Feature Weighting," *Proceedings of the 23rd International Conference on Machine Learning*, Pittsburgh Pennsylvania USA, pp. 913-920, 2006. [CrossRef] [Google Scholar] [Publisher Link]

[37] Casey S. Greene et al., "Spatially Uniform ReliefF (SURF) for Computationally-Efficient Filtering of Gene-Gene Interactions," *BioData Mining*, vol. 2, pp. 1-9, 2009. [CrossRef] [Google Scholar] [Publisher Link]

[38] Casey S. Greene et al., "The Informative Extremes: Using Both Nearest and Farthest Individuals Can Improve Relief Algorithms in the Domain of Human Genetics," *Evolutionary Computation, Machine Learning and Data Mining in Bioinformatics, Lecture Notes in Computer Science*, vol. 6023, pp. 182-193, 2010. [CrossRef] [Google Scholar] [Publisher Link]

[39] Matthew E Stokes, and Shyam Visweswaran, "Application of a Spatially-Weighted Relief Algorithm for Ranking Genetic Predictors of Disease," *BioData Mining*, vol. 5, pp. 1-11, 2012. [CrossRef] [Google Scholar] [Publisher Link]

[40] Delaney Granizo-Mackenzie, and Jason H. Moore, "Multiple Threshold Spatially Uniform ReliefF for the Genetic Analysis of Complex Human Diseases," *Evolutionary Computation, Machine Learning and Data Mining in Bioinformatics, Lecture Notes in Computer Science*, vol. 7833, pp. 1-10, 2013. [CrossRef] [Google Scholar] [Publisher Link]